Pump−Probe Spectroscopy and the Exciton Delocalization Length in Molecular Aggregates

Lisette D. Bakalis and Jasper Knoester*

Institute for Theoretical Physics and Materials Science Center, Nijenborgh 4, 9747 AG Groningen, The Netherlands

Received: February 1, 1999

Using numerical simulations, we investigate to what extent the pump−probe spectrum can be used as a tool to determine the exciton delocalization length in disordered molecular (J) aggregates. We compare the delocalization length obtained through heuristic arguments from the spectral separation between the bleaching and the one- to two-exciton induced absorption features in this spectrum to the delocalization length obtained from the participation ratio at the J band center. We find that up to a certain saturation length these two delocalization lengths are indeed proportional. In the case of long-pulse two-color pump−probe spectra, the slope of this linear scaling is insensitive to the pump frequency; it is sensitive to the width of the probe pulse. Beyond the saturation length, which is determined by the homogeneous line width of the exciton transitions, both the two-color and the short-pulse pump−probe spectra saturate and no longer can be used as a measure for the delocalization length. The latter applies to the B850 ring of bacterial antenna complexes.

I. Introduction

The dynamics of Frenkel excitons in low-dimensional molecular assemblies, like J aggregates[1] and photosynthetic antenna systems,[2] have been the subject of many recent studies. The key quantity that keeps attracting attention is the exciton delocalization length, i.e., the number of molecules over which the exciton's wave function is spread. This length is determined by the competition between the intermolecular excitation transfer interactions and static disorder imposed by the environment (random solvent shifts). At higher temperatures, also inelastic scattering by nuclear motions plays a role (dynamic disorder), which may lead to an exciton mean free path (coherence length) that is shorter than the delocalization length. The amount of exciton delocalization strongly affects the optical response and energy transport properties of the assembly, which explains the considerable interest in this length scale.

Methods to measure the exciton delocalization length make use of collective effects in the optical response. Well-known examples are exciton superradiance[3] and exchange narrowing.[4] Both methods, however, involve uncertainties. In the case of superradiance, the fluorescence quantum yield generally is not known very well, while the use of exchange narrowing requires knowledge of the disorder distribution felt by a single molecule in the aggregate.[5,6]

Recently, the weak-pulse pump−probe spectrum has been used as a third method to determine the delocalization length. For one-dimensional J aggregates, this spectrum contains a negative contribution due to bleaching and stimulated emission of the one-excitons excited by the pump pulse and a blue-shifted positive feature resulting from induced absorption from the excited one-excitons to two-exciton states (see Figure 1).[7−10] The blue shift is a consequence of the fact that two excitations cannot reside on the same molecule (Pauli exclusion),[11] leaving a smaller effective space for the second excitation, which in the case of J aggregates (negative transfer interaction) implies a higher energy. Obviously, this exclusion effect should diminish for larger exciton delocalization size, suggesting, quite generally, a relation between the pump−probe spectrum and the exciton delocalization length.

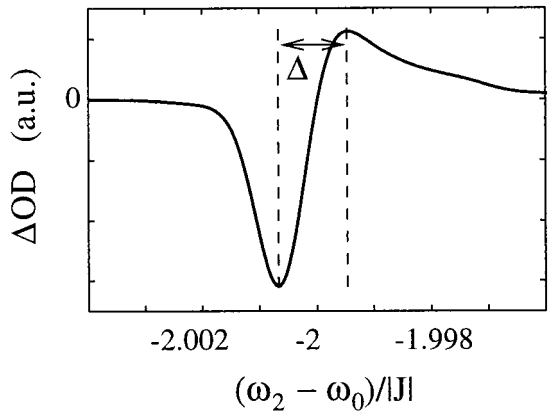

Figure 1. Typical pump−probe spectrum for a J aggregate as a function of the probe frequency ω_2. The spectrum shows a negative contribution due to bleaching and stimulated emission of one-exciton states excited by the pump laser, and a blue-shifted positive feature due to induced absorption from the excited one-exciton to two-exciton states. The spectral separation Δ between both features is thought to be a measure of the exciton delocalization length, a conjecture that is tested in this paper. The spectrum shown here is a two-color pump−probe spectrum simulated for aggregates of 250 molecules with static disorder of strength $\sigma/|J| = 0.01$ (see section III). The pump frequency ω_1 was taken at the maximum of the absorption band.

A more quantitative arguing starts by considering homogeneous one-dimensional aggregates with nearest-neighbor transfer interactions J. The excitons in this system are characterized by a wave number k and an energy $\Omega_k^0 = \omega_0 + 2J\cos(\pi k/(N+1))$, where ω_0 is the single-molecule transition energy and N is the number of molecules in the aggregate (open boundary conditions).[12−14] If N is not too large, one then finds that only two transitions dominate the pump−probe spectrum. The bleaching feature is determined by the superradiant $|k = 1\rangle$ one-exciton state, while the induced absorption is dominated by the transition from this one-exciton to the two-exciton state $|k_1 = 2, k_2 = 1\rangle$.[8,12] Thus, the blue shift Δ between the two features

10.1021/jp990354g CCC: $18.00
Published on Web 07/20/1999

in the pump−probe spectrum is given by[12]

$$\Delta = \Omega^0_{k=2} - \Omega^0_{k=1} \approx 3\pi^2|J|/(N+1)^2 \quad (1)$$

If one now *assumes* that the properties of a disordered aggregate are well-described by those of decoupled homogeneous aggregates with an effective length given by the exciton delocalization length N_{del}, one should replace in eq 1 the physical length N by N_{del}. Inverting the resulting equation, one arrives at a simple expression relating the exciton delocalization length to the observed blue shift in the pump−probe spectrum,

$$N^{pp}_{del} = \sqrt{3\pi^2|J|/\Delta} - 1 \quad (2)$$

where the superscript "pp" has been added to stress the origin (pump−probe) of this length.

As this method to determine the delocalization length has received considerable attention recently,[10,15−17] it should be assessed critically. First, an important step in the above is the replacement of the disordered chain by decoupled homogeneous segments with a low-energy level structure that corresponds to the segment size. Although the numerical simulations of exciton states in ref 18 give some support to this step, a systematic study over a large range of disorder values has not been given. Second, as was pointed out in ref 14, the finite homogeneous line width (γ) of the exciton transitions imposes a natural upper bound on the delocalization length that may be determined from the pump−probe spectrum. When the separation between neighboring one-exciton levels approaches γ, the exciton levels start to mix and the spectrum is no longer dominated by the above two transitions. For homogeneous aggregates, this happens when the aggregate size surpasses the saturation size

$$N_{sat} = \sqrt{3\pi^2|J|/\gamma} - 1 \quad (3)$$

Beyond this size, the pump−probe spectrum should not depend on the delocalization length anymore. Stated differently, the spectrum then gives no information on the delocalization length, but only on the saturation size. Alternatively, one may view N_{sat} as the coherence size of the exciton imposed by the inelastic scattering processes responsible for γ. In fact, Meier, Chernyak, and Mukamel[19] recently stressed that the pump−probe spectrum always measures the coherence size, which in the absence of inelastic scattering equals the delocalization length. They supported their general scaling arguments (relating spectral widths in the presence of scattering to a coherence size) by explicit comparison to a small number (three) of numerical simulations.

In this paper, we report on a systematic study of the effect of exciton delocalization on the pump−probe spectrum of molecular aggregates. We do this by simulating pump−probe spectra for J aggregates with static disorder over a range of disorder strengths. We study the correlation between N^{pp}_{del} determined from these spectra and the "real" delocalization length, N_{del}, which we determine directly from the exciton wave function via the participation ratio.[20,21] In contrast to ref 19, we mainly focus on the *two-color* pump−probe spectrum and we consider the effects of changing the pump frequency and the width of the probe pulse. In all cases, we find a remarkably well-defined linear scaling between the two delocalization lengths as long as N_{del} lies well below the saturation length.

The outline of this paper is as follows. In section II we present the Frenkel exciton Hamiltonian for the aggregate and we discuss a smoothing technique that improves the statistics of the simulated spectra. In section III we give the general expressions for the spectra that we simulate. The results of our simulations for various homogeneous line widths, pump conditions, and probe widths are presented and discussed in section IV. Finally, in section V we conclude.

II. Hamiltonian, Diagonalization, and Smoothing

We consider linear molecular aggregates consisting of a chain of N polarizable two-level molecules labeled n (= 1, ..., N). The molecular transition dipoles all have magnitude μ and equal orientation, so that we may ignore their vector nature. Within the Heitler−London approximation,[22] the Frenkel exciton Hamiltonian for the aggregate reads[23,24]

$$\hat{H} = \sum_{n,m=1}^{N} H_{nm}\hat{b}^\dagger_n\hat{b}_m \quad (4)$$

with the $N \times N$ matrix

$$H_{nm} = (\omega_0 + \epsilon_n)\delta_{n,m} + J(\delta_{n,n-1} + \delta_{n,n+1}) \quad (5)$$

and open boundary conditions. Here, $\hat{b}^\dagger_n$ and $\hat{b}_n$ are the Pauli raising and lowering operators, respectively, for molecular excitations,[23,24] ω_0 denotes the average molecular transition energy ($\hbar = 1$), and J is the nearest-neighbor excitation transfer interaction. Finally, we account for static diagonal disorder through the random energy offsets ϵ_n, which are chosen independently of each other from a Gaussian distribution with standard deviation σ,

$$P(\epsilon_n) = \frac{1}{\sigma\sqrt{2\pi}}\exp(-\epsilon_n{}^2/2\sigma^2) \quad (6)$$

In order to calculate optical spectra using standard sum-over-states expressions,[25,26] one has to diagonalize $\hat{H}$. This is considerably simplified if one uses the Jordan−Wigner transformation from paulions to fermions.[27] As this approach is well-known,[12−14] we only briefly mention the results that are relevant for the remainder of this paper. After the diagonalization, the exciton Hamiltonian obtains the free-fermion form

$$\hat{H} = \sum_{k=1}^{N} \Omega_k\hat{\eta}^\dagger_k\hat{\eta}_k \quad (7)$$

Here, $\hat{\eta}^\dagger_k$ and $\hat{\eta}_k$ are Fermi operators and Ω_k (k = 1, ... , N) is the kth eigenvalue of H_{nm}. The corresponding normalized eigenvector will be denoted $\boldsymbol{\varphi}_k$.

Owing to the fact that quite generally $|J| \ll \omega_0$, the overall ground state $|g\rangle$ of the aggregate is the state in which all molecules are in their respective ground states. The lowest excited states are the one-excitons, in which the molecules share one molecular excitation. They take the form $|k\rangle = \hat{\eta}^\dagger_k|g\rangle$, have energy Ω_k, and transition dipole to the ground state

$$\mu_{gk} = \mu\sum_{n=1}^{N}\varphi_{kn} \quad (8)$$

with φ_{kn} the nth component of the eigenvector $\boldsymbol{\varphi}_k$. The next higher band of excited states is formed by the two-exciton states, $|k_1, k_2\rangle = \hat{\eta}^\dagger_{k_1}\hat{\eta}^\dagger_{k_2}|g\rangle$, with energy $\Omega_{k_1,k_2} = \Omega_{k_1} + \Omega_{k_2}$. Two-excitons cannot be excited directly from the ground state.

The transition dipole between $|k_1, k_2\rangle$ and the one-exciton state $|k\rangle$ is given by

$$\mu_{k,k_1k_2} = \mu \sum_{n_2>n_1} (\varphi_{kn_1} + \varphi_{kn_2})(\varphi_{k_1n_1}\varphi_{k_2n_2} - \varphi_{k_1n_2}\varphi_{k_2n_1}) \quad (9)$$

We finally note that higher exciton bands exist, but those are not relevant for the weak-pulse pump−probe spectrum (or for any other third-order nonlinear optical technique). This follows from the fact that only transitions between adjacent multiexciton bands are dipole allowed.

In the general case of disorder, one has to resort to simulations in order to calculate "exact" spectra. For each randomly generated disorder realization, H_{nm} is diagonalized numerically, from which the multiexciton energies and transition dipoles follow. This has to be repeated many times in order to obtain smooth spectra. Depending on the particular parameter values, however, the statistics of the spectra may be improved considerably by applying a smoothing technique that was proposed by Makhov et al.[28] for the linear absorption spectrum. In the following, we outline this technique from a more general point of view.

The generic form of spectral functions is

$$I(\omega) = \langle \sum_k F(\boldsymbol{\varphi}_k)\, f(\omega - \Omega_k) \rangle \quad (10)$$

Here, $\langle ... \rangle$ stands for the average over $\epsilon_1, ..., \epsilon_N$. Furthermore, F is a function of the eigenvectors and f is a broadening function that, for instance, accounts for the finite homogeneous line widths of the exciton transitions. As a specific example, for the linear absorption spectrum we have $F = \mu^2|\sum_n \varphi_{kn}|^2$ and f is a Lorentzian with half-width at half-maximum (HWHM) γ. Similarly, for the density of one-exciton states, $F = 1$. For nonlinear optical spectra, F may take more complicated forms (see below). It is now obvious that if the disorder strength σ is large compared to the width of f ($\sigma \gg \gamma$), one has to sample many disorder realizations to obtain a smooth spectrum. Under these conditions, the smoothing technique of ref 28, which was introduced for the extreme case of $\gamma = 0$ ($f(\omega - \Omega_k) = \delta(\omega - \Omega_k)$), is most useful.

The crux of this technique is that it samples the disorder realizations more efficiently by allowing for an analytical averaging over the mean value $\bar{\epsilon} = \sum_n \epsilon_n/N$ of the N random offsets in one chain. For small chains, the fluctuations in this mean offset are important limitations to obtaining good statistics in numerical simulations. Technically, the separation of $\bar{\epsilon}$ is achieved by expressing the random offsets in a new set of random variables $\epsilon'_1, ..., \epsilon'_N$ using the orthonormal transformation

$$\epsilon_n = \sum_{m=1}^{N} c_{nm}\epsilon'_m \quad (11)$$

with

$$c_{nm} = \frac{1}{\sqrt{N}}\left[\sin\left(\frac{2\pi}{N}(n-1)(m-1)\right) + \cos\left(\frac{2\pi}{N}(n-1)(m-1)\right)\right] \quad (12)$$

The orthonormality guarantees that $\sum_n \epsilon_n^2 = \sum_m (\epsilon'_m)^2$, implying that the ϵ'_m obey the same independent Gaussian statistics as the original offsets. Furthermore, from the inverse transformation, $\epsilon'_n = \sum_{m=1}^{N} c_{mn}\epsilon_m$, one observes that $\epsilon'_1 = \sqrt{N}\bar{\epsilon}$; i.e., ϵ'_1 describes the mean of the original random offsets.

Using this transformation, the average over ϵ'_1 may indeed be carried out explicitly. To this end, consider the special case[28] of the average eq 10 with $f(\omega - \Omega_k) = \delta(\omega - \Omega_k)$,

$$\begin{aligned} I_0(\omega) &= \langle \sum_k F(\boldsymbol{\varphi}_k)\, \delta(\omega - \Omega_k) \rangle \\ &= \int d\epsilon_1 ... \int d\epsilon_N \prod_n P(\epsilon_n) \sum_k F(\boldsymbol{\varphi}_k)\, f(\omega - \Omega_k) \\ &= \int d\epsilon'_1 ... \int d\epsilon'_N \prod_n P(\epsilon'_n) \sum_k F(\boldsymbol{\varphi}_k)\, f(\omega - \Omega_k) \end{aligned} \quad (13)$$

The last expression seems not very useful, as the Ω_k and the $\boldsymbol{\varphi}_k$ are the eigenvalues and eigenvectors of H_{nm}, which is defined in terms of the ϵ_n and not of the ϵ'_n. Let us define, however, the new matrix H'_{nm} similar to eq 5, except that ϵ_n is replaced by

$$\sum_{m=2}^{N} c_{nm}\epsilon'_m = \epsilon_n - \epsilon'_1/\sqrt{N} \quad (14)$$

(cf. eqs 11 and 12). Thus, we effectively subtracted the mean value $\bar{\epsilon}$ of the original offsets from all the molecular transition frequencies. Let the eigenvalues and eigenvectors of H'_{nm} (which is determined completely by $\epsilon'_2, ..., \epsilon'_N$) be denoted Ω'_k and $\boldsymbol{\varphi}'_k$. Obviously, $\Omega'_k = \Omega_k - \epsilon'_1/\sqrt{N}$ and $\boldsymbol{\varphi}'_k = \boldsymbol{\varphi}_k$, as $H'_{nm} = H_{nm} - \epsilon'_1/\sqrt{N}\,\delta_{nm}$. Thus the last form of eq 13 may be rewritten,

$$I_0(\omega) = \int d\epsilon'_1 ... \int d\epsilon'_N \prod_n P(\epsilon'_n) \sum_k F(\boldsymbol{\varphi}'_k)\, \delta\left(\omega - \Omega'_k - \frac{\epsilon'_1}{\sqrt{N}}\right) \quad (15)$$

In this form, the integration over ϵ'_1 is easily performed by eliminating the delta function, leading to

$$I_0(\omega) = \sqrt{\frac{N}{2\pi\sigma^2}} \left\langle \sum_k F(\boldsymbol{\varphi}'_k) \exp\left(\frac{-N(\omega - \Omega'_k)^2}{2\sigma^2}\right) \right\rangle' \quad (16)$$

where the average $\langle ... \rangle'$ is performed over the $N-1$ Gaussian variables $\epsilon'_2, ..., \epsilon'_N$.

Returning to our original average of interest, $I(\omega)$, we note that this is simply related to $I_0(\omega)$ by

$$I(\omega) = I_0(\omega) \otimes f(\omega) \quad (17)$$

where $\otimes$ denotes a convolution ($\int d\omega' I_0(\omega') f(\omega - \omega')$). Thus, at the price of an extra convolution, it is always possible to sample the mean value of the original offsets analytically. In practice, one now simulates the remaining average eq 16; i.e., one randomly chooses $\epsilon'_2, ..., \epsilon'_N$, calculates H'_{nm}, and diagonalizes this matrix in order to obtain Ω'_k and $\boldsymbol{\varphi}'_k$. Repeating this many times gives $I_0(\omega)$, which after the fast convolution of eq 17 results in the desired average of eq 10.

The improvement of the statistics (leading to smoother spectra) is recognized in eq 16 from the fact that a series of δ functions, occurring in the original average of $I_0(\omega)$, is replaced by a series of Gaussians with the finite width $\sigma/\sqrt{N}$. Of course, for the actual function of interest, $I(\omega)$, this method only constitutes an improvement as long as $\sigma/\sqrt{N} > \gamma$. It thus depends on the parameter values and chain size whether it is profitable to use the smoothing technique.

We finally note that for nonlinear spectra, the function F in eq 10 may be more complicated and depend on all eigenvectors as well as on the eigenvalues, $F(\{\boldsymbol{\varphi}'_q\}, \{\Omega'_q\})$. The above derivation then results in the same expression, except that in eq 16

$$F(\boldsymbol{\varphi}'_k) \rightarrow F(\{\boldsymbol{\varphi}'_q\}, \{\Omega'_q - \Omega'_k + \omega\}) \tag{18}$$

III. General Expressions for the Spectra

In this section, we give the explicit expressions which we used as the basis for our simulations. First, we discuss the participation ratio. This well-known measure for the energy-dependent delocalization size of a particle (exciton in our case) in the presence of disorder is defined as[20,21,29]

$$\boldsymbol{P}(\omega) = \frac{\langle \sum_k \delta(\omega - \Omega_k)\rangle}{\langle \sum_k (\sum_n \varphi_{kn}{}^4)\delta(\omega - \Omega_k)\rangle} \tag{19}$$

$\boldsymbol{P}(\omega)$ measures the number of molecules that on the average participate in the states that occur at energy ω. This is seen by considering the two limiting situations. For states that are completely localized on one molecule we have $\sum_n(\varphi_{kn})^4 = 1$, leading to $\boldsymbol{P}(\omega) = 1$ at the frequency of the state. On the other hand, for the completely delocalized states that exist on perfectly ordered chains ($\varphi_{kn} \sim \sin(\pi kn/(N+1))$), one has $\sum_n(\varphi_{kn})^4 = 3/(2(N+1))$,[20,29] giving $\boldsymbol{P}(\omega) = 2(N+1)/3$. This motivates one to define the frequency dependent delocalization length as

$$N_{\mathrm{del}}(\omega) = \frac{3}{2}\boldsymbol{P}(\omega) - 1 \tag{20}$$

The behavior of the participation ratio as a function of energy has been studied in various papers[21,29] and agrees with the general picture that states close to the center of the one-exciton band stay more delocalized in the presence of disorder than states close to the band edges.[30] Near the J band (the main absorption band which for $\sigma \leq |J|$ occurs in a narrow region at the lower exciton band edge), the energy dependence of $\boldsymbol{P}(\omega)$ is rather strong.[21,29] In particular, the participation ratio decreases when moving from the blue side to the red side of the J band, indicative of the growing localization when one moves further away from the center of the exciton band.

We note that it is trivial to apply the smoothing procedure introduced in the previous section to both disorder averages in eq 19. For the numerator, one finds eq 16 with $F = 1$, while $F = \sum_n(\varphi'_{kn})^4$ for the denominator.

We next turn to the optical spectra. Although our focus is on the pump−probe spectrum, we will also need the linear absorption spectrum, in order to determine at what frequency to pump when simulating two-color pump−probe experiments. The sum-over-states expression for the linear absorption spectrum reads[25,26]

$$A(\omega) = \left\langle \sum_k |\mu_{gk}|^2 \frac{\gamma}{(\omega - \Omega_k)^2 + \gamma^2} \right\rangle \tag{21}$$

with γ the homogeneous line width of the transition from the ground state to the one-exciton, which is assumed independent of k. Again, it is straightforward to apply the smoothing procedure of the previous section, leading to

$$A(\omega) = \sqrt{\frac{N}{2\pi\sigma^2}}\left\langle \sum_k |\mu_{gk}|^2 \exp\left(\frac{-N(\omega - \Omega'_k)^2}{2\sigma^2}\right)\right\rangle' \otimes L(\omega) \tag{22}$$

with $L(\omega) \equiv \gamma/(\omega^2 + \gamma^2)$.

For the pump−probe spectrum, we distinguish between the case where the pump and probe laser pulses are spectrally narrow compared to the J band and the case where they are broad. The first case applies to two-color (long-pulse) pump−probe spectroscopy, while the second applies to ultrashort laser pulses. In both cases, we will assume that the pulses are weak, so that, neglecting coherent artifacts,[26] the experiment can be separated in two linear absorption processes. In the first, the pump excites the aggregate into a one-exciton state; in the second process, the excited one-exciton state is probed by measuring the linear absorption of the probe. This gives rise to three contributions: (i) stimulated emission at the frequency of the excited one-exciton state; (ii) bleaching (reduced absorption) of all one-exciton states; (iii) induced absorption from the excited one-exciton to two-exciton states. In the difference absorption spectrum ΔOD, (i) and (ii) give negative peaks (often simply referred to as "bleaching"), while (iii) leads to positive features.

We first consider the two-color pump−probe spectrum, in which we have narrow pump and probe pulses with central frequencies ω_1 and ω_2, respectively. The line shape functions of these pulses around their central frequencies are denoted $\hat{I}_{\mathrm{pu}}(\omega)$ and $\hat{I}_{\mathrm{pr}}(\omega)$, respectively. Thus, $\hat{I}_{\mathrm{pu}}(\omega)$ and $\hat{I}_{\mathrm{pr}}(\omega)$ both have their maximum at $\omega = 0$ and widths that are given by the inverse pulse duration. The pulses are narrow compared to the linear absorption band of the aggregate. Under these conditions, the probe absorption spectrum, measured as the total power absorption from the probe pulse, is given by[5]

$$\Delta\mathrm{OD}(\omega_1,\omega_2) = -\int \mathrm{d}\omega'_1 \int \mathrm{d}\omega'_2\, \hat{I}_{\mathrm{pu}}(\omega_1 - \omega'_1)\, \hat{I}_{\mathrm{pr}}(\omega_2 - \omega'_2) \times \left\langle \sum_k \frac{|\mu_{gk}|^2\gamma}{(\omega'_1 - \Omega_k)^2 + \gamma^2} \left\{ \sum_{k'} [1 + \delta_{k,k'}] \frac{|\mu_{gk'}|^2\gamma}{(\omega'_2 - \Omega_{k'})^2 + \gamma^2} - \sum_{k_1 > k_2} \frac{|\mu_{k,k_1k_2}|^2\gamma'}{(\omega'_2 + \Omega_k - \Omega_{k_1} - \Omega_{k_2})^2 + (\gamma')^2} \right\} \right\rangle \tag{23}$$

The first term in curly brackets describes the bleaching and the stimulated emission, while the second term gives the induced absorption. As before, γ is the homogeneous width of the ground state to one-exciton transitions and γ' is the width of the one-exciton to two-exciton transitions. The integrations over ω'_1 and ω'_2 account for the convolutions of the pulse shapes with the homogeneous line shapes of the various exciton transitions. In the Appendix, we give the expression that follows from eq 23 after smoothing.

Finally, we consider the short-pulse pump−probe experiment, where the laser pulses are much broader than the aggregate absorption band. In this case, the pump pulse excites all one-exciton states with a probability proportional to their oscillator strengths, but independent of their transition energies. The probe absorption spectrum is resolved by a monochromator. The

general expression for the thus obtained differential absorption reads[14]

$$\Delta\mathrm{OD}(\omega) = -\left\langle \sum_k \frac{[N\mu^2 + |\mu_{gk}|^2]|\mu_{gk}|^2\gamma}{(\omega - \Omega_k)^2 + \gamma^2} \right\rangle + \left\langle \sum_k \sum_{k_1>k_2} \frac{|\mu_{gk}\mu_{k,k_1k_2}|^2\gamma'}{(\omega + \Omega_k - \Omega_{k_1} - \Omega_{k_2})^2 + (\gamma')^2} \right\rangle \quad (24)$$

After applying the smoothing procedure, this expression leads to eq 28 of the Appendix.

IV. Results and Discussion

In this section, we present and discuss the results of our numerical simulations. All calculations were done on chains of $N = 250$ molecules with $J < 0$ (J aggregates). The disorder strength σ was varied from $0.001|J|$ to $0.3|J|$. For each disorder value, 500 randomly generated disorder realizations were sampled, resulting in smooth spectra. Three values of the homogeneous one-exciton line width have been chosen: $\gamma = 0, 5 \times 10^{-4}|J|$, and $8 \times 10^{-4}|J|$, respectively. The last two values are typical for the homogeneous line width of PIC J aggregates in a low-temperature glassy host.[31] For the line width of the one- to two-exciton transition, we used $\gamma' = 3\gamma$. This relaxation model applies if the molecules of the aggregate each have a bilinear coupling to a bath with short correlation time, which may be considered independent for different molecules.[32] This model also yields the assumed k independence of the various decay rates. Using eq 3, the two nonzero values for γ yield saturation lengths of 240 and 190 molecules, respectively.

A. Linear Absorption Spectrum. The linear absorption spectrum was simulated using eq 22. The main reason for calculating this spectrum is that we needed it for the two-color pump−probe spectrum, where we used pump frequencies and laser line widths defined relative to the maximum and the width of the J band (the main absorption band), respectively. A secondary reason is that the linear spectrum provided a check on our numerical procedure, as this spectrum has been thoroughly studied before. In particular, we checked the conservation of oscillator strength and the behavior of the absorption spectrum with changing disorder strength. As is well-known, with increasing disorder, the J band broadens and its maximum shifts to the red. For intermediate disorder strength, such that $N \gg N_{\mathrm{del}} \gg 1$, the width of the J band scales like $\sigma^{4/3}$. This has been found from numerical simulations as well as from analytical approaches.[29,33−36] In the strong- and weak-disorder limits, however, this scaling breaks down. For strong disorder, one approaches the molecular limit ($N_{\mathrm{del}} \equiv 1$), where the J band width is proportional to σ. For very weak disorder ($N_{\mathrm{del}} \approx N$), one reaches the exchange (or motional) narrowing limit, where the J band width scales like $\sigma/\sqrt{N}$.[4,5] Thus, the width of the absorption band behaves like σ^x, where x changes from 1 to 4/3 and back to 1 with increasing σ. The σ values where these changes occur depend on the aggregate size N, as observed by Makhov et al.,[28] although we believe them to occur more smoothly than found by these authors. For $N = 250$ and varying σ from $0.001|J|$ to $0.3|J|$, we found a smooth change of x from 1.09 to 1.30. This is in agreement with the above. The larger disorder values used in our simulations ($\sigma/|J| = 0.06\cdots0.3$) lie in the intermediate regime and yield exciton delocalization lengths (obtained from the participation ratio at the J band maximum) on the order of 50 molecules.

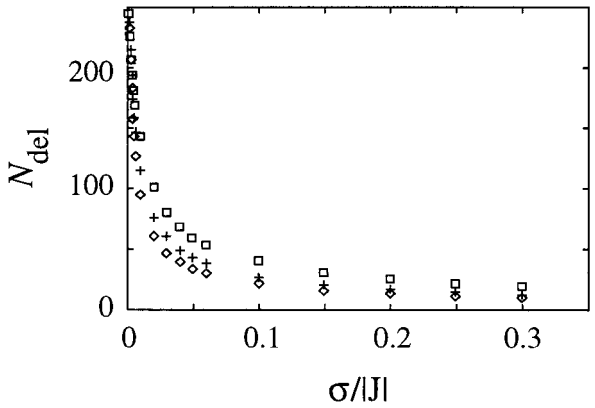

Figure 2. Exciton delocalization length calculated from the participation ratio (eq 20) as a function of the disorder strength. The participation ratio was calculated at three different energies: at the red half-maximum of the J band (◇), at the center of the J band (+), and at the blue half-maximum of the J band (□).

B. Participation Ratio. In order to have a reference value for the exciton delocalization length that is directly obtained from the wave function (and not from a particular observable), we calculated the participation ratio. Figure 2 gives the thus obtained delocalization length as a function of disorder for three different energies: (i) ω_c, the position of the center (maximum) of the J band simulated at the same disorder; (ii) ω_r, the position of the red half-maximum of this band; (iii) ω_b, the position of the blue half-maximum. We note that these energies are not fixed in an absolute sense, because the position and width of the J band depend on the disorder strength.

As expected, we find that at all energies, $N_{\mathrm{del}} \rightarrow N$ in the limit of small disorder, while N_{del} decreases with growing disorder strength. At the same time, the figure shows that for fixed disorder the delocalization length decreases with lowering energy, which agrees with the well-known fact that localization is stronger when one moves away from the center of the one-particle band (see discussion below eq 20). As long as the delocalization length is small compared to the aggregate size N, its values at different frequencies turn out to be linearly related to each other. In particular, we find that for $N \leq 80$, $N_{\mathrm{del}}(\omega_r) = 0.80N_{\mathrm{del}}(\omega_c) - 0.63$, while $N_{\mathrm{del}}(\omega_b) = 1.35N_{\mathrm{del}}(\omega_c) + 3.0$.

C. Two-Color Pump−Probe Spectrum. Using the expressions given in section III, we simulated two-color pump−probe spectra under various conditions. For the central frequency ω_1 of the pump laser, we considered the three choices ω_c, ω_r, and ω_b, defined in section IV.B. Hereafter, we will refer to these pump choices as "central excitation", "red excitation", and "blue excitation", respectively.

We first discuss simulations in which we minimized the effect of laser pulse widths. This was achieved by choosing a δ-function probe, while for the pump pulse we used a Gaussian with a standard deviation $\sigma_{\mathrm{pu}} = 0.3W$, where W is the half-width at half maximum of the J band simulated at the same disorder strength. For smaller pump widths, the statistics of the simulated spectra deteriorate too much, due to the fact that most simulated aggregates do not have a one-exciton that can be excited by the narrow pump. In these simulations, we used the smoothing technique (i.e., eq 27). A typical example of a thus obtained two-color pump−probe spectrum is shown in Figure 1.

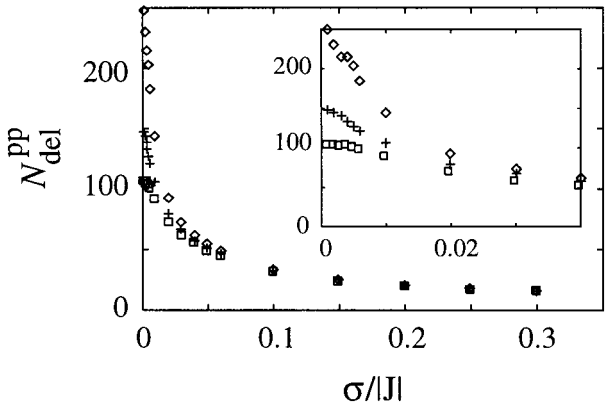

Figure 3. Effective exciton delocalization length N_{del}^{pp}, obtained through eq 2 from simulated two-color pump−probe spectra, as a function of the disorder strength. The pump frequency was taken at the center of the J band ($\omega_1 = \omega_c$) and a δ probe pulse was used. Different symbols refer to the three different values of the homogeneous line width: $\gamma = 0$ (◇), $5 \times 10^{-4}|J|$ (+), and $8 \times 10^{-4}|J|$ (□). The inset shows a blowup of the small-disorder part of the plot.

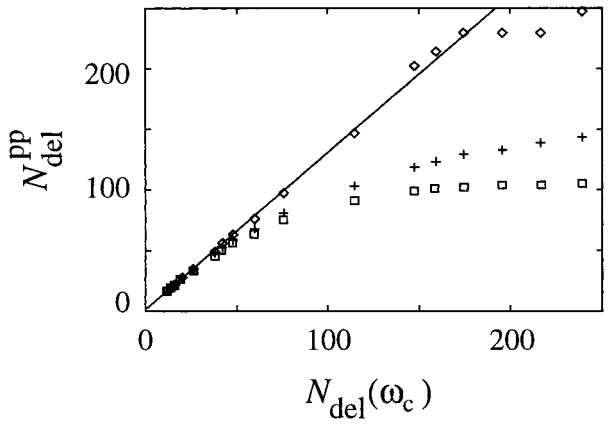

Figure 4. Exciton delocalization length obtained from the simulated two-color pump−probe spectrum after pumping at the J band center, plotted against the delocalization length calculated from the participation ratio at the J band center. A δ-shaped probe pulse was used and a Gaussian pump pulse with a width of 0.3 times the HWHM of the J band. Data points represent $\gamma = 0$ (◇), $5 \times 10^{-4}|J|$ (+), and $8 \times 10^{-4}|J|$ (□), respectively. The solid line is the best linear fit through the first eight data points for $\gamma = 0$; its slope and abscissa can be found in Table 1.

For each disorder strength, we determined from the simulated spectrum the separation Δ between the maxima of the bleaching and induced absorption features, and derived the exciton delocalization length N_{del}^{pp} according to eq 2. For vanishing homogeneous line width ($\gamma = 0$), this length qualitatively follows the same behavior as observed for the real delocalization length in Figure 2. In the homogeneous limit $N_{del}^{pp} \rightarrow N$, while for increasing disorder N_{del}^{pp} decreases monotonously. Inclusion of a finite line width γ, however, alters this behavior. With decreasing disorder, N_{del}^{pp} is first found to follow the $\gamma = 0$ data and then starts to level off at a value that depends on γ. This is shown in Figure 3 for the case of central excitation.

This behavior is easily understood. If the disorder strength is rather large, inclusion of a finite γ value does not affect the pump−probe spectrum (and N_{del}^{pp}), simply because all spectral features then have widths that are dominated by the static disorder. The smaller the disorder strength gets, however, the more important the homogeneous broadening becomes. This broadening leads to a growing overlap of the negative bleaching and the blue-shifted positive induced absorption peaks. Due to this overlap, these features partially cancel each other in the total spectrum, a phenomenon that leads to an apparent increase in the observed value for Δ. As a consequence, N_{del}^{pp} decreases (cf. eq 2). This is the precursor of the size saturation mentioned in section I. Lowering the disorder even further, eventually brings one to the saturated spectrum, which is insensitive to a further decrease of the disorder or, alternatively stated, to a further increase of the delocalization length N_{del}. Therefore, the highest value for N_{del} that can be measured using the pump−probe spectrum depends on the homogeneous line width of the excitons and should be expected to be on the order of N_{sat} defined in eq 3.

In order to see how well N_{del}^{pp} reflects the real delocalization length N_{del}, we plotted the former against the latter, so that each data point gives the pair (N_{del}, N_{del}^{pp}) for one value of the disorder strength. Figure 4 gives the thus obtained plot for the case of central excitation, where we used the participation ratio at the absorption line center. Moving from left to right in this figure, the data points correspond to a decreasing disorder strength ($0.3|J|-0.001|J|$). For $\gamma = 0$ a surprisingly good linear relation between both values of the delocalization length is found, which extends to delocalization lengths of more than 100 molecules (i.e., half the physical chain length). The best linear fit (accounting for data points up to $N_{del} = 50$) yields

$$N_{del}^{pp} = aN_{del}(\omega_c) + b \tag{25}$$

with $a = 1.29$ and $b = 1.72$. Extending the fit region up to $N_{del} = 150$ only gives minor changes in these coefficients ($a = 1.28$, $b = 2.11$). The accuracy of the fits indicates that the pump−probe spectrum under these conditions indeed is a good tool to measure the delocalization length.

On the other hand, Figure 4 clearly shows that for finite γ the linear scaling breaks down due to the saturation effect. N_{del}^{pp} obtained from the pump−probe spectrum levels off, while the real delocalization length continues to increase. We observe that for the γ values used, the same linear scaling as for $\gamma = 0$ is obeyed up to $N_{del} \approx 50$, which is well below the saturation size; i.e., the precursor to saturation is notable at an early stage. Finally, it is important to note that the observed linear scaling at small delocalization lengths is not particular for the system size of $N = 250$ molecules. We performed the same simulations for aggregates of $N = 80$ molecules and found that for N_{del} up to roughly 50 molecules, the data accurately follow the same linear scaling. For larger delocalization lengths (smaller disorder), finite size effects occur in the $N = 80$ chain.

We followed the same procedure as above for pump−probe spectra obtained with red and blue excitation. The comparison between the thus obtained delocalization lengths and the real delocalization length *at the J band center* is plotted in Figures 5 and 6, respectively. Again, for delocalization lengths of up to more than 100 molecules, linear scalings are found, with slopes (a) and abscissae (b) that are given in Table 1. As above, finite γ values cause the scaling to break down around $N_{del} = 50$. It is remarkable that the slopes are equal (within their error bars of 3%) for all three excitation frequencies considered here. This implies that, independent of the pump frequency, the two-color spectrum measures the delocalization length at the J band center (since we used this as a common reference). This, in turn, also implies that the two-color pump−probe spectrum cannot be used in a straightforward way to map out the energy dependence of the delocalization length in the J band.

In fact, it turns out that over a large range of disorder values, a linear relation holds between Δ and W (the HWHM of the J

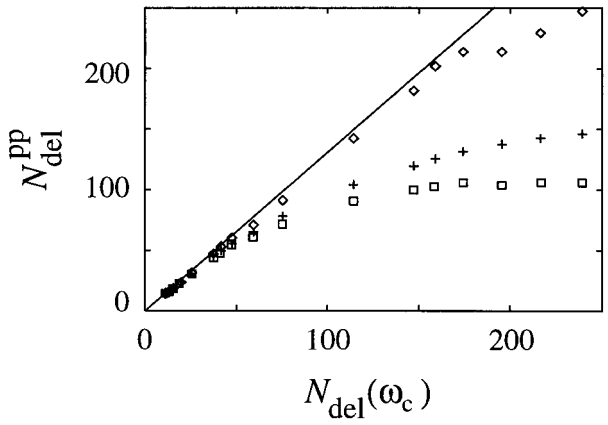

Figure 5. As figure 4, but now the pump frequency is at the red half-maximum of the J band. The participation ratio is still taken at the J band center.

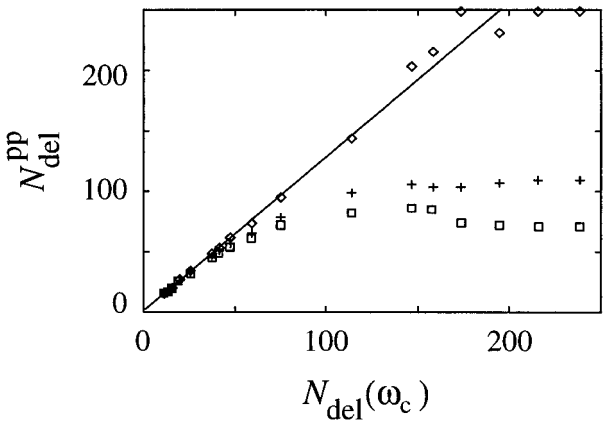

Figure 6. As figure 4, but now with pump frequency at the blue half-maximum of the J band. The participation ratio is still taken at the J band center.

TABLE 1: Coefficients *a* (Slope) and *b* (Abscissa) for the Linear Fits (Eq 25) of the relation between the Delocalization Length Obtained from Two-Color Pump−Probe Spectroscopy and the Delocalization Length Obtained from the Participation Ratio at the Center of the J Band[a]

	δ-probe			finite probe		
	red	center	blue	red	center	blue
a	1.31	1.29	1.28	0.96	1.09	1.03
b	0.24	1.72	1.43	0.55	0.33	1.12

[a] Distinction is made between probe pulses that are δ shaped or that have a finite width (HWHM of 0.3 times the HWHM of the linear absorption spectrum). In both cases, three positions of the narrow pump pulse are considered: at the red half-maximum, the center, and the blue half-maximum of the J band. Four of the fits are displayed in figures 4−7 along with the simulated data. In all cases, the fit was obtained by considering data points with $N_{del} \leq 50$. The slopes are only slightly changed if the fitted interval is extended to $N_{del} = 150$ ($\leq$5% for all cases, except for the last column, where finite size effects cause larger inaccuracies, cf. discussion in section IV.D).

band),

$$\Delta = cW \tag{26}$$

with $c \approx 0.8$, independent of the pump-frequency. The constant c, however, changes when the homogeneous line width approaches the disorder strength; i.e., eq 26 is not universal. Using analytical arguments, Meier et al.[19] have suggested a similar scaling for the case of short pump pulses, leading to $c = 2/\sqrt{3} \approx 1.15$. The numerical results reported by these authors also indicate that this scaling is not universal.

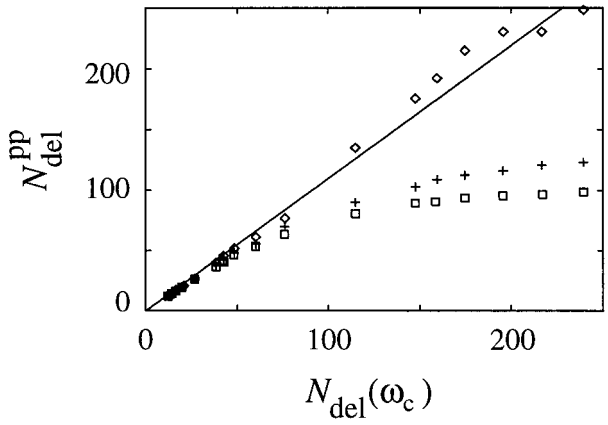

Figure 7. As figure 4, but now with Lorentzian pump and probe pulses, both with a HWHM of 0.3 times the HWHM of the J band.

We now turn to pump−probe spectra where both the pump and probe pulses have a finite width. For this case, we used Lorentzian pump and probe pulses with a HWHM of $\Gamma = 0.3W$, where W is the HWHM of the J band simulated at the same disorder strength as the pump−probe spectrum. The Lorentzian pulse shapes were used for convenience, as they allow for analytical evaluation of the integrals over ω_1' and ω_2' in eq 23. We did not use the smoothing procedure in these calculations.

We followed the same procedure as in the case of δ probes and compared N_{del}^{pp} obtained from the pump−probe spectra to $N_{del}(\omega_c)$ obtained from the participation ratio at the J band center. The results are similar to the ones for δ probes and we only give the plot for the case of central excitation (Figure 7). The slopes and abscissae for the corresponding linear relations are given in Table 1. We note that the slopes are smaller than in the case of the δ probes and that they have larger mutual differences. The fact that the slopes are smaller can be understood from the fact that the introduction of a finite probe width is equivalent to keeping a δ probe while increasing the homogeneous line widths γ and γ' in the second transition in eq 23 (caused by the probe pulse) to $\gamma + \Gamma$ and $\gamma' + \Gamma$, respectively. This broadening of the transitions gives rise to an increased overlap of positive and negative features in the pump−probe spectrum, which, in analogy to the precursor of saturation, leads to a larger apparent Δ value and, thus, to a smaller value for N_{del}^{pp}. As the extra width Γ decreases for smaller disorder strength (as W then becomes smaller), the effect does not lead to real saturation in the case of $\gamma = 0$, but merely to a lowering of the slope a.

If eq 26 were universal, i.e., held for an arbitrary ratio of disorder strength and homogeneous line width, we could use the above noted equivalence between a finite probe width and increasing the homogeneous line width to derive the approximate dependence of the slope a on the probe width. For the probe width $\Gamma = \kappa W$, this leads to $a(\kappa) = a(\kappa = 0)/\sqrt{1+\kappa}$. For our case of $\kappa = 0.3$, this gives a reduction of 12% in the slope a with respect to the case of a δ probe, which is about half of the real reduction seen in Table 1. We attribute this discrepancy mainly to the fact that eq 26 is nonuniversal.

D. Short Pulse Pump−Probe Spectrum. Using eq 28, we conducted a study similar to the ones in section IV.C for the case of short pump and probe pulses. In this case, no pump and probe frequencies or widths can be varied, so that we do not have to distinguish various cases, as we did for the two-color spectra. Again, we studied the relation between the

delocalization length obtained from the pump−probe spectrum and the one obtained from the participation ratio at the center of the J band. As before, we found the linear relation eq 25 to be obeyed for small delocalization lengths, where the best fit for $N_{del} < 50$ yields a slope $a = 0.84$ and abscissa $b = 0.70$. It should be pointed out, however, that this linear scaling breaks down around $N_{del} = 100$, even for $\gamma = 0$. Repeating our calculations for various smaller chain sizes N, clearly indicates that this breakdown is due to finite-size effects. These effects occur rather early for this case, as the broad pump pulse also excites states that occur on the (far) blue side of the J band, where the delocalization length is considerably larger than at the J band center (cf. section IV.B). This early onset of finite-size effects probably also is the cause of the reduced accuracy for the case of the blue excitation two-color pump−probe spectrum with finite probe width.

V. Concluding Remarks

In this paper, we have numerically assessed the possibility of using the pump−probe spectrum as a tool to determine the exciton delocalization length in aggregates with diagonal disorder. Considering various excitation and probing conditions, we have shown that, as long as static disorder dominates over homogeneous broadening, the pump−probe spectrum, using eq 2, gives a delocalization length N_{del}^{pp} proportional to the real delocalization length $N_{del}(\omega_c)$ (obtained from the participation ratio at the J band center). Dynamic effects (homogeneous broadening) limit the delocalization lengths that may be determined this way to values smaller than $\sim 0.3N_{sat}$, where the saturation size is defined in eq 3. As discussed in the Introduction, this saturation size may also be interpreted as the exciton coherence size imposed by inelastic scattering.

We have shown that for two-color pump−probe spectroscopy with δ-shaped probe pulses, the coefficients in the relation $N_{del}^{pp} = aN_{del}(\omega_c) + b$ are practically independent of the pump frequency ($a \approx 1.3$, while $b = O(1)$). This is rather surprising, because the participation ratio has a strong energy dependence within the J band. This implies on the one hand that the typical delocalization length may accurately be measured with the pump−probe spectrum, but on the other hand, that its energy dependence apparently cannot be determined this way. We have also seen that increasing the width of the probe pulse leads to a smaller slope a, an effect that is well-understood (section IV.C). As long as the probe pulse is narrower than the J band, however, the slope stays close to unity. The latter also seems to hold for short-pulse pump−probe spectra, although finite size effects at present make it impossible to determine the linear scaling for this case over a large interval of delocalization lengths.

In our study, we have used values for the homogeneous line widths that are typical for excitons in J aggregates of pseudoisocyanine (PIC) at low temperature (1.5 K).[31] These line widths are rather small, which explains why the linear scaling holds up to the large delocalization length of $N_{del} \approx 50$. This interval is large enough to accurately determine the delocalization length in PIC from pump−probe spectra, as this length is estimated from other methods to be in the order of 50 molecules.[37] On the other hand, for the hotly debated example of the B850 ring in the light-harvesting complex (LH2) of purple bacteria, the homogeneous line width is generally believed to be much larger, even at low temperature: $\gamma/|J| \approx 0.5$.[38−40] This leads to a saturation size of only about eight molecules, which means that the linear scaling probably breaks down around 2 or 3 molecules already. In other words, the length scale of 4 ± 2 molecules determined from the pump−probe spectrum on the LH2 system[17] is not the delocalization length imposed by static disorder but is to a large extent determined by the homogeneous broadening, i.e., by dynamic effects. This agrees with the findings of Meier et al.[19] and Jimenez et al.[40]

In our model Hamiltonian, we have not included exciton−exciton interactions, which in principle may be of importance when dealing with multiexciton manifolds, as they may lead to bound biexcitons[41,42] and exciton−exciton annihilation.[43−46] It is known, however, that over a large range of interaction strengths, the effect on the pump−probe spectrum is rather small.[41] Interestingly, for homogeneous aggregates, the effect of strong interactions may be accounted for by replacing the physical aggregate size by a slightly smaller effective size.[42] It remains to be seen whether an analogue of this, such as an apparent small change of the delocalization length, occurs in the presence of disorder.

We finally note that our results have important implications concerning the issue of intermolecular correlations of the diagonal disorder in molecular aggregates. In ref 5, it was shown that the spectral separation between the bleaching and the induced absorption contributions *before adding them to form the total spectrum* contain information on such correlations. In particular, the dependence of this separation on the pump frequency is stronger for decreasing correlations. Experimentally, this dependence was found to be very weak, leading to surprisingly large estimates of the disorder correlation length of 50−100 molecules for PIC aggregates[6] and several hundred molecules for TDBC aggregates.[16] Our numerical results show, however, that even for completely uncorrelated disorder the separation Δ between the bleaching and the induced absorption in the *total* spectrum is totally insensitive to the pump frequency (over the interval considered). This is clear from the fact that the slope a is insensitive to the pump frequency. Therefore, obtaining information on the correlation length from experimental spectra, which necessarily are *total* spectra, relies on a delicate deconvolution into separate bleaching and induced absorption contributions. This introduces considerable uncertainties, raising doubts whether the large correlation lengths reported so far indeed exist or just are an artifact of the method involved.

Acknowledgment. The authors thank Professor F. C. Spano for many stimulating discussions.

Appendix

In this Appendix, we give the expressions for the pump−probe spectra after applying the smoothing method outlined in section II. We first consider the two-color pump−probe spectrum eq 23. In the first term (bleaching and stimulated emission), we take $f = \gamma/((\omega_2' - \Omega_{k'})^2 + \gamma^2)$, while in the second term (induced absorption), we take $f = \gamma'/((\omega_2' + \Omega_k - \Omega_{k_1} - \Omega_{k_2})^2 + (\gamma')^2)$. The latter is slightly more complicated than the standard situation considered in section II, as f involves three fermion frequencies, instead of one. However, after transformation to the new variables ϵ_n', the combination $\Omega_k - \Omega_{k_1} - \Omega_{k_2}$ yields one net term $-\epsilon_1'/\sqrt{N}$, just like it occurs in the δ function in eq 15, which allows for straightforward generalization of the standard approach. We then find

$$\Delta\mathrm{OD}(\omega_1,\omega_2) = -\sqrt{\frac{N}{2\pi\sigma^2}} \int \mathrm{d}\omega_1' \int \mathrm{d}\omega_2' \, \hat{I}_{\mathrm{pu}}(\omega_1 - \omega_1') \, \hat{I}_{\mathrm{pr}}(\omega_2 - \omega_2') \times \left[\left\langle \sum_{k,k'} \frac{[1+\delta_{k,k'}]|\mu_{gk}\,\mu_{gk'}|^2\gamma}{(\omega_1' - \omega_2' - \Omega_k' + \Omega_{k'}')^2 + \gamma^2} \times \exp\left(\frac{-N}{2\sigma^2}(\omega_2' - \Omega_{k'}')^2\right) \right\rangle' \otimes L(\omega_2') - \left\langle \sum_k \sum_{k_1>k_2} \frac{|\mu_{gk}\,\mu_{k,k_1k_2}|^2\gamma}{(\omega_1' - \omega_2' - 2\Omega_k' + \Omega_{k_1}' + \Omega_{k_2}')^2 + \gamma^2} \times \exp\left(\frac{-N}{2\sigma^2}(\omega_2' + \Omega_k' - \Omega_{k_1}' - \Omega_{k_2}')^2\right) \right\rangle' \otimes L'(\omega_2') \right] \quad (27)$$

with L defined below eq 22 and L' the same Lorentzian with γ replaced by γ'.

Applying the smoothing method to the short-pulse pump−probe spectrum eq 24 works in a completely analogous way and leads to

$$\Delta\mathrm{OD}(\omega) = -\sqrt{\frac{N}{2\pi\sigma^2}} \left\langle \sum_k [N\mu^2 + |\mu_{gk}|^2]|\mu_{gk}|^2 \exp\left(\frac{-N}{2\sigma^2}(\omega - \Omega_k')^2\right) \right\rangle' \otimes L(\omega) + \sqrt{\frac{N}{2\pi\sigma^2}} \left\langle \sum_k \sum_{k_1>k_2} |\mu_{gk}\,\mu_{k,k_1k_2}|^2 \times \exp\left(\frac{-N}{2\sigma^2}(\omega + \Omega_k' - \Omega_{k_1}' - \Omega_{k_2}')^2\right) \right\rangle' \otimes L'(\omega) \quad (28)$$

References and Notes

(1) For a recent overview, see: *J-aggregates*, Kobayashi, T., Ed.; World Scientific: Singapore, 1996.

(2) Hu, X.; Schulten, K. *Phys. Today* **1997**, *50*, 28 and references therein.

(3) Boer, S. de; Vink, K. J.; Wiersma, D. A. *Chem. Phys. Lett.* **1987**, *137*, 99.

(4) Knapp, E. W. *J. Chem. Phys.* **1983**, *85*, 73.

(5) Knoester, J. *J. Chem. Phys.* **1993**, *99*, 8466.

(6) Durrant, J. R.; Knoester, J.; Wiersma, D. A. *Chem. Phys. Lett.* **1994**, *222*, 450.

(7) Gadonas, R.; Danielius, R.; Piskarskas, R.; Rentsch, S. *Izv. Akad. Nauk. SSSR Fiz.* **1983**, *47*, 2445; *Bull. Akad. Sci. USSR Phys.* **1983**, *47*, 151.

(8) Fidder, H.; Knoester, J.; Wiersma, D. A. *J. Chem. Phys.* **1993**, *98*, 6563.

(9) Johnson, A. E.; Kumazaki, S.; Yoshihara, K. *Chem. Phys. Lett.* **1993**, *211*, 511.

(10) Minoshima, K.; Taiji, M.; Misawa, K.; Kobayashi, T. *Chem. Phys. Lett.* **1994**, *218*, 67.

(11) Spano, F. C.; Mukamel, S. *Phys. Rev. Lett.* **1991**, *66*, 1197.

(12) Juzeliūnas, G. *Z. Phys. D* **1988**, *8*, 379.

(13) Spano, F. C. *Phys. Rev. Lett.* **1991**, *67*, 3424.

(14) Knoester, J.; Spano, F. C. In *J-aggregates*; Kobayashi, T., Ed.; World Scientific: Singapore, 1996 (see also references therein).

(15) Burgel, M. van; Wiersma, D. A.; Duppen, K. *J. Chem. Phys.* **1995**, *102*, 20.

(16) Moll, J.; Daehne, S.; Durrant, J. R.; Wiersma, D. A. *J. Chem. Phys.* **1995**, *102*, 6362.

(17) Pullerits, T.; Chachisvilis, M.; Sundström, V. *J. Phys. Chem.* **1996**, *100*, 10787.

(18) Malyshev, V.; Moreno, P. *Phys. Rev. B* **1995**, *51*, 14587.

(19) Meier, T.; Chernyak, V.; Mukamel, S. *J. Phys. Chem. B* **1997**, *101*, 7332.

(20) Thouless, D. J. *Phys. Rep.* **1974**, *13*, 93.

(21) Schreiber, M.; Toyozawa, Y. *J. Phys. Soc. Jpn.* **1982**, *51*, 1537.

(22) Bakalis, L. D.; Knoester, J. *J. Chem. Phys.* **1997**, *106*, 6964.

(23) Davydov, A. S. *Theory of Molecular Excitons*; Plenum: New York, 1971.

(24) Agranovich, V. M.; Galanin, M. D. In *Electronic Excitation Energy Transfer in Condensed Matter*; Agranovich, V. M., Maradudin, A. A., Eds.; North-Holland: Amsterdam, 1982.

(25) Boyd, R. W. *Nonlinear Optics*; Academic Press: New York, 1992.

(26) Mukamel, S. *Principles of Nonlinear Optical Spectroscopy*; Oxford: Oxford, U.K., 1995.

(27) Jordan, P.; Wigner, E. *Z. Phys.* **1928**, *47*, 631.

(28) Makhov, D. V.; Egorov, V. V.; Bagatur'yants, A. A.; Alfimov, M. V. *Chem. Phys. Lett.* **1995**, *246*, 371.

(29) Fidder, H.; Knoester, J.; Wiersma, D. A. *J. Chem. Phys.* **1991**, *95*, 7880.

(30) Economou, E. N. *Green's Functions in Quantum Physics*; Springer: Berlin, 1990.

(31) Fidder, H.; Knoester, J.; Wiersma, D. A. *Chem. Phys. Lett.* **1990**, *171*, 529.

(32) Leegwater, J. A.; Mukamel, S. *Phys. Rev. A* **1992**, *46*, 452.

(33) Schreiber, M.; Toyozawa, Y. *J. Phys. Soc. Jpn.* **1982**, *51*, 1528.

(34) Köhler, J.; Jayannavar, A. M.; Reineker, P. *Z. Phys. B* **1989**, *75*, 451.

(35) Boukahil, A.; Huber, D. L. *J. Lumin.* **1990**, *45*, 13.

(36) Malyshev, V. A. *J. Lumin.* **1993**, *55*, 225.

(37) Fidder, H. Collective optical response of molecular aggregates. Ph.D. Thesis, University of Groningen, 1993.

(38) Reddy, N. R. S.; Picorel, R.; Small, G. J. *J. Phys. Chem.* **1992**, *96*, 6458.

(39) Leupold, D.; Voigt, B.; Pfeiffer, M.; Bandilla, M.; Scheer, H. *Photochem. Photobiol.* **1993**, *57*, 24.

(40) Jimenez, R.; van Mourik, F.; Fleming, G. R. *J. Phys. Chem. B* **1997**, *101*, 7350.

(41) Spano, F. C. *Chem. Phys. Lett.* **1995**, *234*, 29.

(42) Juzeliūnas, G.; Reineker, P. *J. Chem. Phys.* **1997**, *107*, 9801; **1998**, *109*, 6916.

(43) Sundström, V.; Gillbro, T.; Gadonas, R. A.; Piskarskas, A. *J. Chem. Phys.* **1988**, *89*, 2754.

(44) Knoester, J.; Spano, F. C. *Phys. Rev. Lett.* **1995**, *74*, 2780.

(45) Malyshev, V. A.; Glaeske, H.; Feller, K.-H. *J. Lumin.* **1998**, *76/77*, 455.

(46) Valkunas, L.; Trinkunas, G.; Liuolia, V. In *Resonance Energy Transfer*; Andrews, D. L., Demidov, A. A., Eds.; Wiley: New York, 1999.